

Article

A New GNSS Single-Epoch Ambiguity Resolution Method Based on Triple-Frequency Signals

Shengli Wang ^{1,2}, Jian Deng ³, Xiushan Lu ¹, Ziyuan Song ² and Ying Xu ^{2,*}

¹ Institute of Ocean Engineering, Shandong University of Science and Technology, Qingdao 266590, China; shlwang@sdust.edu.cn (S.W.); xiushanl@vip.sina.com (X.L.)

² College of Geomatics, Shandong University of Science and Technology, Qingdao 266590, China; SKDSZY0228@163.com

³ School of Computer and Information Engineering, Xiamen University of Technology, Xiamen 361024, China; dengjian163@126.com

* Correspondence: yingxu@sdust.edu.cn; Tel.: +86-532-8605-7276

Academic Editors: Zhao-Liang Li, Jose A. Sobrino, Chao Ren and Wolfgang Kainz

Received: 17 November 2016; Accepted: 10 February 2017; Published: 18 February 2017

Abstract: Fast and reliable ambiguity resolution (AR) has been a continuing challenge for real-time precise positioning based on dual-frequency Global Navigation Satellite Systems (GNSS) carrier phase observation. New GNSS systems (i.e., GPS modernization, BDS (BeiDou Navigation Satellite System), GLONASS (Global Navigation Satellite System), and Galileo) will provide multiple-frequency signals. The GNSS multiple-constellation and multiple-frequency signals are expected to bring great benefits to AR. A new GNSS single-epoch AR method for a short-range baseline based on triple-frequency signals is developed in this study. Different from most GNSS multiple-constellation AR methods, this technique takes advantage of the triple-frequency signals and robust estimation as much as possible. In this technique, the double difference (DD) AR of the triple-frequency observations is achieved in the first step. Second, the triple-frequency carrier phase observations with fixed ambiguities are used with the dual-frequency carrier phase observations to estimate their ambiguity. Finally, to realize reliable GNSS single-epoch AR, robust estimation is involved. The performance of the new technique is examined using 24 hours of GPS/GLONASS/BDS observation collected from a short-range baseline. The results show that single-epoch AR of the GNSS signals can be realized using this new technique. Moreover, the AR of BDS Geostationary Earth Orbit (GEO) satellites' observations is easier than are those of the Medium Earth Orbit (MEO) and Inclined Geosynchronous Satellite Orbit (IGSO) satellites' observations.

Keywords: GNSS; ambiguity resolution; single-epoch; multiple-constellation; triple-frequency signal; short-range baseline

1. Introduction

Centimetre-level accuracy positioning can be achieved using the Global Navigation Satellite Systems (GNSS) carrier phase observation, which has been used in military and civilian fields [1–3]. To satisfy centimetre-level accuracy positioning requirements, the carrier Network Real-Time Kinematic (NRTK) positioning technology technique is commonly used. One key issue of the carrier phase-based real-time positioning technique is to fix the ambiguity On The Fly (OTF) [4]. Generally, the goal of OTF AR (ambiguity resolution) is to resolve ambiguities both correctly and as quickly as possible in terms of both the time span of observations and the computation time. OTF AR requires good station–satellite geometry and a low level of observation errors and biases. Moreover, it requires a fast and reliable algorithm. Over the past several decades, numerous AR algorithms have been developed. The most famous ones are the least-squares ambiguity search technique (LSAST) [5], the fast AR

approach (FARA) [6], the fast ambiguity search filter (FASF) [7] and the least-squares ambiguity decorrelation adjustment method (LAMBDA) [8,9]. LAMBDA is currently a popular method both theoretically and practically among the ambiguity determination methods; it significantly reduces the computational complexity of the ambiguity search stage and has promoted the development of RTK in the 20th century. Precise point positioning (PPP) [10] is another popular technique for precise positioning based on carrier phase observation. However, approximately 15 min is needed to achieve reliable integer ambiguity solutions. To take advantage of both PPP and NRTK, several methods have been developed to improve the performance of PPP services in specific areas by using regional reference networks [11–13]. To achieve instantaneous ambiguity resolution, a new strategy was proposed [14]. In the proposed method, precise zero-differenced atmospheric delays are derived from the PPP fixed solution of the reference stations, which are disseminated to and interpolated at user stations to correct for L1 or L2 phase observations or their combination. With the corrected observations, instantaneous ambiguity resolution can be achieved, thus achieving the position solutions equivalent to the network RTK.

With the development of GPS, BDS, GLONASS and Galileo, GNSS is entering a new era. GNSS multiple-constellation and multiple-frequency signals will bring both opportunities and challenges to the fast AR. Most research [15,16] has shown that the initialization and the centimetre-level position can be obtained in a very short time by using multiple-frequency observations. Li [17] clearly showed that the fusion of multiple GNSS significantly increases the number of observed satellites, optimizes the spatial observation geometry at a site, and improves the convergence, accuracy, continuity and reliability of positioning. In detail, the addition of the BDS, Galileo and GLONASS systems to the standard GPS-only processing reduces the convergence time by almost 70% and improves the positioning accuracy by approximately 25%. Research also shows that the GLONASS and BDS have the potential capability for real-time atmospheric parameter retrieval for time-critical meteorological applications as GPS does, and that the combination of multi-GNSS observations can improve the performance of a single-system solution in meteorological applications, with higher accuracy and robustness [18].

Three/Multiple-Carrier AR (TCAR/MCAR) [16] and Cascading Integer Resolution (CIR) [19] are the typical three/multiple-carrier AR methods. Both TCAR and CIR use the same geometry-free model to fix the ambiguities with a three- or four-step rounding procedure that is biased by the residual ionospheric delay. Following this study, a large amount of work has been carried out regarding triple-frequency AR using the TCAR/CIR or modified TCAR/CIR methods. Feng and Li [20] used both a geometry-based and geometry-free TCAR model to process the ambiguity resolution. A geometry- and ionosphere-free distance-independent reliable TCAR method was proposed in 2010 by Li et al. [21]; it was free of both ionospheric effects and geometric terms. Ji et al. [22] presented an improved CAR method that includes the advantages of both integer least-squares (ILS) and CAR. Geng and Bock [23] proposed a method where the incoming triple-frequency GPS signals are exploited to enable rapid convergences to ambiguity-fixed solutions in real-time precise point positioning (PPP). Tang et al. [24] proposed a modified stepwise AR method based on the TCAR and evaluated its performance using real BDS data. The LAMBDA method's application to the multi-frequency AR problem has been studied extensively by a number of research groups [24–26]. LAMBDA can be applied to either multi-frequency geometry-free cases or multi-frequency geometry-based cases. The algorithms mentioned above can all be used for the AR of multi-constellation and multi-frequency signals. However, most of the AR algorithms mentioned above simply combine different systems together without bringing every single system's superiority into full play. In this paper, we focus on this issue.

This paper focuses on fixing the ambiguity of GNSS carrier phase observation based on the triple-frequency signals in real time. The mathematical model applied in this study is introduced in the second section. Section three introduces the new GNSS single-epoch AR method. The performance of this method is tested based on GNSS observation; the test results are shown in Section 4. Finally, there is a conclusion.

2. Mathematical Model

GPS, BDS and Galileo signals are code division multiple access (CDMA) signals. Ignoring the multipath, their double difference (DD) pseudo-range and carrier phase measurements can be formulated as [27]

$$\nabla\Delta P_i = \nabla\Delta\rho + \nabla\Delta\frac{K}{f_i^2} + \nabla\Delta T + \nabla\Delta\varepsilon_{i,P} \quad (1)$$

$$\nabla\Delta\lambda_i\phi_i = \nabla\Delta\rho + \lambda_i\nabla\Delta N_i - \nabla\Delta\frac{K}{f_i^2} + \nabla\Delta T + \nabla\Delta\varepsilon_{i,\phi} \quad (2)$$

where $\nabla\Delta$ —DD operator;

i —the i -th frequency, e.g., GPS L1, L2 or L5;

f —frequency (Hz);

P —pseudo-range measurements (meter);

ϕ —carrier phase measurements (cycle);

λ —wavelength (meter);

ρ —geometric distance from satellite to receiver (meter);

N —carrier phase ambiguity;

K —the parameter of the first-order ionospheric delay, $K = 40.28$ TEC; TEC represents the Total Electron Content;

T —tropospheric delay (meter);

$\varepsilon_{i,P}, \varepsilon_{i,\phi}$ —measurement noise of pseudo range and carrier phase, respectively.

In contrast to GPS/BDS/Galileo, GLONASS uses frequency division multiplexing (FDMA—frequency division multiple access) to make the signals from individual satellites distinguishable. Because of FDMA, GLONASS carrier phase and pseudo-range observations suffer from inter-channel biases (ICBs). The effects of receiver ICBs are different from channel to channel of the same receiver and cannot be eliminated by the basic DD technique [28]. Additionally, receiver ICBs in code and carrier phase measurements are different. However, the GLONASS AR process is more complicated compared to GPS because of the FDMA signal structure. At least one GLONASS satellite participates in the DD observation, the wavelengths are no longer identical, and Equation (2) can no longer be simplified in this way without losing the integer characteristic of the ambiguity terms. Therefore, single difference terms remain in the DD observation equation. Forming DD carrier phase observations between users and satellites i and j , the GLONASS observation equation becomes

$$\nabla\Delta P_i = \nabla\Delta\rho + \nabla\Delta\frac{K}{f_i^2} + \nabla\Delta T + \nabla\Delta d_{i,P} + \nabla\Delta\varepsilon_{i,P} \quad (3)$$

$$\phi_i = \nabla\Delta\rho + \lambda_i^j\nabla\Delta N + (\lambda_i^j - \lambda_i^r)\Delta N^r - \nabla\Delta\frac{K}{f_i^2} + \nabla\Delta T + \nabla\Delta d_{i,\phi} + \nabla\Delta\varepsilon_{i,\phi} \quad (4)$$

In the equations, Δ —Single difference operator—ICBs for two receivers on adjacent GLONASS pseudo-range and carrier phase observation (meter).

The majority of studies reveal that receivers of the same type have almost the same ICBs. As a consequence, ICBs can be eliminated by a single difference between satellites [28]. However, ICBs should be calibrated before the AR of GLONASS for the relative positioning with different types of receivers [29].

In this study, we focus only on the short-range baseline, and most of the ionospheric delay and the tropospheric delay can be eliminated by DD. Consequently, Equations (1) and (2) can be rewritten as

$$\nabla\Delta P_i = \nabla\Delta\rho + \nabla\Delta\varepsilon_{i,P} \quad (5)$$

$$\nabla \Delta \lambda_i \phi_i = \nabla \Delta \rho + \lambda_i \nabla \Delta N_i + \nabla \Delta \varepsilon_{i,\phi} \quad (6)$$

The general form of the linear observation equation on GNSS carrier phase observations can be re-expressed as [3]

$$AX + BN + \varepsilon = L \quad (7)$$

where L denotes the DD observation vector, N is the DD carrier phase integer ambiguity vector ($N \in Z^n$), X is the vector of other unknown parameters (including position coordinates), ε is the random errors, and the matrices A and B are the corresponding design matrices. Note that we only use the carrier phase observation to estimate the float solution of the rover in this paper. The detailed methodology will be introduced in the next section.

The solution of Equation (7) can be obtained by minimizing Equation (8):

$$\min \|L - BN - AX\|_{Q_L}^2, \quad N \in Z^n, X \in R^n \quad (8)$$

where $\|*\|_{Q_L}^2 = (*)^T Q_L^{-1} (*)$ and Q_L is the variance–covariance (VC) matrix of observation vector L .

In general, the fixed solution can be divided into three steps. In the first step, the integer constraints on the ambiguities are simply ignored. The unconstrained least-squares solution is referred to as the float solution of \hat{N} , \hat{X} and the corresponding variance–covariance matrix, as follows

$$\begin{bmatrix} \hat{N} \\ \hat{X} \end{bmatrix}, \quad \begin{bmatrix} Q_{\hat{N}} & Q_{\hat{N}\hat{X}} \\ Q_{\hat{X}\hat{N}} & Q_{\hat{X}} \end{bmatrix} \quad (9)$$

In the second step, the integer ambiguity estimation \check{N} is computed from the “float” ambiguity, subject to $\min \|\hat{N} - \check{N}\|_{Q_{\hat{N}}}^2$. This can be efficiently done using the LAMBDA method. Finally, a fixed solution is obtained by

$$\check{X} = \hat{X} - Q_{\hat{X}\hat{N}} Q_{\hat{N}}^{-1} (\hat{N} - \check{N}) \quad (10)$$

3. GNSS Single-Epoch Ambiguity Resolution

Single-epoch AR has been a continuing challenge for GNSS dual-frequency bands, even under a short-range baseline. Fortunately, triple- or even multiple-frequency signals form an extra-wide-lane and wide-lane combination, the ambiguities of which can be fixed much more easily based on the relatively large wavelength. BDS is currently a unique system that provides triple-frequency signals. However, the visible BDS satellites may be not sufficient to estimate the position of the rover in a high-rise-intensive city. Another situation would be that the geometry of the visible triple-frequency satellites constellation may be not sufficiently strong to obtain a precise position. For instance, if all of the visible BDS satellites were the GEO satellites, the constellation geometry would be too weak to compute a precision position. To fix the ambiguities of GNSS signals and provide a positioning and navigation service for the rover in a short time, a new single-epoch GNSS AR method for a short-range baseline based on triple-frequency signals is developed in this study. The theory and steps of this method are (Figure 1) as follows:

Step 1. As the first operational system with triple-frequency bands, the ambiguities of BDS signals can be fixed faster than the other GNSS signals. In the first step, we fix the ambiguities of BDS EWL(Extra Wide Lane) and B1 signals; the detailed methodology is introduced in Section 3.1.

Step 2. After the ambiguities of the BDS signals, we estimate the float solution by using the BDS carrier phase (B1) observation with fixed ambiguity and other satellites’ carrier phase observation (L1). This step is discussed in detail in Section 3.2.

Step 3. Finally, to realize reliable AR for the GNSS carrier phase observation, robust estimation is involved (Section 3.3).

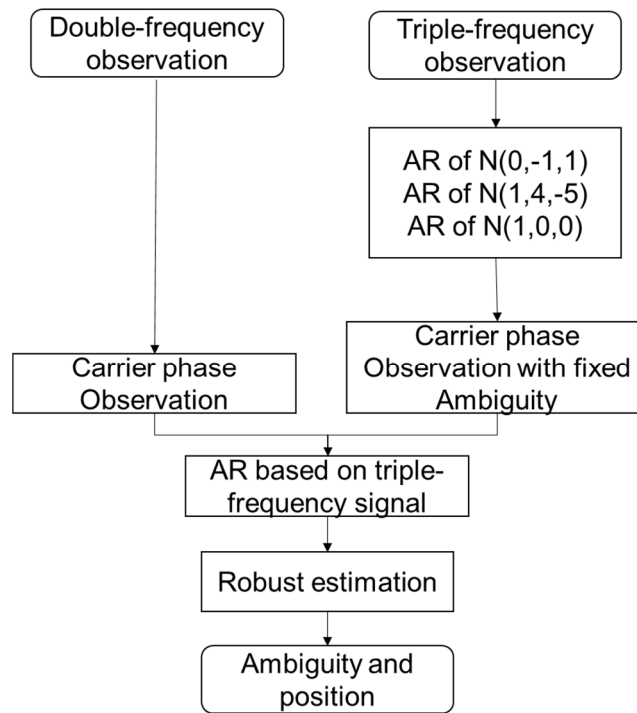


Figure 1. Structure of the new single-epoch Global Navigation Satellite Systems ambiguity resolution (GNSS AR) method for a short-range baseline based on triple-frequency signals.

3.1. Ambiguity Resolution of BDS Triple-Frequency Signals

Supposing that there are three carrier phase frequencies f_1, f_2, f_3 , the general form of linear observation equations for the GNSS pseudo-range and carrier phase observation combination can be expressed as Equations (11) and (12) (unit: metre). Although most of the atmospheric effects in the code and carrier phase observation can be cancelled by DD, the linear combination may increase these effects. Thus, the tropospheric delay and the ionospheric delay still exist in the observation combination equation below.

$$\nabla\Delta\Phi_{(i,j,k)} = \nabla\Delta\rho + \nabla\Delta T - \beta_{(i,j,k)} \frac{\nabla\Delta K}{f_1^2} - \lambda_{(i,j,k)} \nabla\Delta N_{(i,j,k)} + \nabla\Delta\varepsilon_{\Phi_{(i,j,k)}} \quad (11)$$

$$\nabla\Delta P_{(m,n,l)} = (m + n + l)(\nabla\Delta\rho + \nabla\Delta T) + \beta_{(m,n,l)} \frac{\nabla\Delta K}{f_1^2} + \nabla\Delta\varepsilon_{P_{(m,n,l)}} \quad (12)$$

where

$$\nabla\Delta\Phi_{(i,j,k)} = \frac{i \cdot f_1 \cdot \nabla\Delta\Phi_1 + j \cdot f_2 \cdot \nabla\Delta\Phi_2 + k \cdot f_3 \cdot \nabla\Delta\Phi_3}{i \cdot f_1 + j \cdot f_2 + k \cdot f_3} \quad (13)$$

$$\nabla\Delta P_{(m,n,l)} = m \nabla\Delta P_1 + n \nabla\Delta P_2 + l \nabla\Delta P_3 \quad (14)$$

where $\nabla\Delta\Phi_{(i,j,k)}$ and $\nabla\Delta P_{(m,n,l)}$ are the DD carrier phase and pseudo-range observation combination in metres, respectively. i, j, k are the combination coefficients, which are integers. m, n, l are the corresponding combination coefficients, which are real numbers. The corresponding ambiguity, virtual frequency and wavelength of the combination is

$$\nabla\Delta N_{(i,j,k)} = i \cdot \nabla\Delta N_1 + j \cdot \nabla\Delta N_2 + k \cdot \nabla\Delta N_3 \quad (15)$$

$$f_{(i,j,k)} = i \cdot f_1 + j \cdot f_2 + k \cdot f_3 \quad (16)$$

$$\lambda_{(i,j,k)} = \frac{c}{f_{(i,j,k)}} = \frac{\lambda_1 \lambda_2 \lambda_3}{i \cdot \lambda_2 \lambda_3 + j \cdot \lambda_1 \lambda_3 + k \cdot \lambda_1 \lambda_2} \quad (17)$$

c denotes the speed of light. λ_i and N_i indicate the wavelength and ambiguities of each carrier phase observation.

The combined ionospheric delay factor is

$$\beta_{(i,j,k)} = \frac{f_1^2 \left(\frac{i}{f_1} + \frac{j}{f_2} + \frac{k}{f_3} \right)}{f_{(i,j,k)}} \quad (18)$$

The DD combination observation noise is

$$\nabla \Delta \varepsilon_{\Phi_{(i,j,k)}} = \frac{i \cdot f_1 \nabla \Delta \varepsilon_{\Phi_1} + j \cdot f_2 \nabla \Delta \varepsilon_{\Phi_2} + k \cdot f_3 \nabla \Delta \varepsilon_{\Phi_3}}{f_{(i,j,k)}} \quad (19)$$

Due to the large wavelength, the ambiguity of the extra-wide lane of $\nabla \Delta N_{(0,1,-1)}$, $\nabla \Delta N_{(1,4,-5)}$ can be fixed using (take the extra-wide lane of BDS as an example)

$$\nabla \Delta N_{(0,1,-1)} = \left[\frac{\nabla \Delta P_{(0,1,-1)} - \nabla \Delta \Phi_{(0,1,-1)}}{\lambda_{(0,1,-1)}} \right] \quad (20)$$

$$\nabla \Delta N_{(1,4,-5)} = \left[\frac{\nabla \Delta P_{(1,0,0)} - \nabla \Delta \Phi_{(1,4,-5)}}{\lambda_{(1,4,-5)}} \right] \quad (21)$$

where $[]$ represents the rounding-off operator.

The standard deviation of the estimated ambiguities should be

$$\sigma_{\Delta \nabla N_{(0,1,-1)}} = \frac{1}{\lambda_{(0,1,-1)}} \sqrt{\sigma_{\Delta \nabla P_2}^2 + \sigma_{\Delta \nabla P_3}^2 + \sigma_{\Delta \nabla \Phi_2}^2 + \sigma_{\Delta \nabla \Phi_3}^2} \quad (22)$$

$$\sigma_{\Delta \nabla N_{(1,4,-5)}} = \frac{1}{\lambda_{(1,4,-5)}} \sqrt{\sigma_{\Delta \nabla P_1}^2 + \sigma_{\Delta \nabla \Phi_1}^2 + 4^2 \sigma_{\Delta \nabla \Phi_2}^2 + 5^2 \sigma_{\Delta \nabla \Phi_3}^2 + (0.3479 \cdot \Delta \nabla I)^2} \quad (23)$$

Assuming that the triple-frequency code and carrier phase observations have the same standard deviations (STD),

$$\sigma_{\nabla \Delta \phi} = \sigma_{\nabla \Delta \phi_1} = \sigma_{\nabla \Delta \phi_2} = \sigma_{\nabla \Delta \phi_3} = 0.01 \text{ m} \quad (24)$$

$$\sigma_{\nabla \Delta P_1} = \sigma_{\nabla \Delta P_2} = \sigma_{\nabla \Delta P_3} = \sigma_{\nabla \Delta P} = 0.5 \text{ m} \quad (25)$$

Under the circumstances of a short-range baseline, we can set the DD ionospheric error ($\Delta \nabla I$ in Equation (23)) to be 10 cm [30]. According to the error propagation, the standard deviation of the estimated ambiguity is 0.148 cycle and 0.172 cycle, respectively. Consequently, relatively reliable ambiguities of the extra-wide lanes can be fixed using the rounding method in a single epoch.

After the AR of the extra-wide lane, we can use $\nabla \Delta \Phi_{(0,1,-1)}$ and $\nabla \Delta \Phi_{(1,0,0)}$ to fix the ambiguity $\nabla \Delta N_{(1,0,0)}$. However, this combination amplifies the observation noise and the ionospheric delay residual, which will significantly affect the ambiguity resolution. To overcome these issues, we chose $\nabla \Delta \Phi_{(1,-1,0)}$; its ambiguity can be calculated as $\nabla \Delta N_{(1,-1,0)} = -5 \nabla \Delta N_{(0,1,-1)} + \nabla \Delta N_{(1,4,-5)}$. Thus, we have

$$\begin{cases} \nabla \Delta \Phi_{(1,-1,0)} = \Delta \nabla \rho + \Delta \nabla \delta_{trop} - \beta_{(1,-1,0)} \frac{\Delta \nabla K}{f_1^2} - \lambda_{(1,-1,0)} \Delta \nabla N_{(1,-1,0)} + \Delta \nabla \varepsilon_{\Phi_{(1,-1,0)}} \\ \nabla \Delta \Phi_{(1,0,0)} = \Delta \nabla \rho + \Delta \nabla \delta_{trop} - \beta_{(1,0,0)} \frac{\Delta \nabla K}{f_1^2} - \lambda_{(1,0,0)} \Delta \nabla N_{(1,0,0)} + \Delta \nabla \varepsilon_{\Phi_{(1,0,0)}} \end{cases} \quad (26)$$

Then, the ambiguity can be expressed as

$$\nabla\Delta N_{(1,0,0)} = \frac{\nabla\Delta\Phi_{(1,-1,0)} - \nabla\Delta\Phi_{(1,0,0)} + \lambda_{(1,-1,0)}\nabla\Delta N_{(1,-1,0)}}{\lambda_{(1,0,0)}} \quad (27)$$

where $\nabla\Delta\phi_{(1,-1,0)}$ and $\nabla\Delta\phi_{(1,0,0)}$ are the DD carrier phase observation of the two wide-lane combinations in metres, $\Delta\nabla\delta_{trop}$ is the DD tropospheric delay, $\frac{\Delta\nabla K}{f_1^2}$ is the ionospheric delay, and β , λ , $\Delta\nabla N$, and $\Delta\nabla\varepsilon$ are the mapping function, wavelength, DD ambiguity and the observation noise of the two wide-lane combinations, respectively.

In this combination, the standard deviation of the estimated ambiguity is only 0.209 cycle. Thus, the success rate of the AR of $\nabla\Delta\Phi_{(1,0,0)}$ is also very high in theory.

3.2. GNSS Ambiguity Resolution under the Constraint of BDS Triple-Frequency Observation

Now, we classify the ambiguities of GNSS observation into two categories. One is the ambiguity ($\nabla\Delta N_e$) of the BDS three-frequency signal, which was resolved in the last section. The other is the ambiguity ($\nabla\Delta N_h$) of the other GNSS satellites' double-frequency observation, which is relatively difficult to resolve. The error equation of the GNSS observation can be expressed as follows:

$$\begin{pmatrix} V_1 \\ V_2 \end{pmatrix} = \begin{pmatrix} A_1 & O \\ A_2 & C_2 \end{pmatrix} \begin{pmatrix} X' \\ \nabla\Delta N_h \end{pmatrix} - \begin{pmatrix} L_1 - C_1\nabla\Delta N_e \\ L_2 \end{pmatrix} \quad (28)$$

V_1 , V_2 are the residual of BDS and the GNSS observations, respectively. X' is the vector of unknown parameters of the coordinate. $\nabla\Delta N_e$ and $\nabla\Delta N_h$ are the ambiguities of the BDS B1 observation and the other GNSS L1 observations. L_1 , L_2 are the carrier phase observation of BDS (B_1) and the GNSS observations (L_1), respectively. A_1 , A_2 and C_1 , C_2 are the corresponding coefficient matrices. Generally, Equation (28) can be simplified to

$$V_k = A_k X_k - L_k \quad (29)$$

where V_k is the matrix of observation residuals and A_k is the coefficient matrix of the parameters. Then, the least-squares solution is

$$\widehat{X}_k = \left(A_k^T P A_k \right)^{-1} A_k^T P L_k \quad (30)$$

In Equation (28), we involve the ambiguity of BDS, which can be fixed more easily than that of GNSS dual-frequency signals. Then, the first part of this equation is free from the effect of ambiguity, which is a restriction of this model and will increase the efficiency of the AR of the GNSS carrier phase observation.

3.3. GNSS Single-Epoch Ambiguity Resolution Based on Robust Estimation

The algorithm mentioned above can yield the GNSS single-epoch AR over a short-range baseline. However, the AR success rate of BDS carrier phase observation is not 100%. The mis-fixing ambiguity will certainly bring an error to the tropospheric delay used to restrict the GPS/GLONASS observation equation. Moreover, it is difficult to avoid the effect of gross observational error on the data processing. In this study, to overcome the issues mentioned above, a robust estimation is used. The effect of these errors is rejected by using a reasonable weight.

According to the theory of robust estimation, the M estimation is

$$\widehat{X}_{kM} = \left(A_k^T \bar{P} A_k \right)^{-1} A_k^T \bar{P} L_k \quad (31)$$

where \bar{P} represents the equal weight matrix. The common equal weight functions include the Huber weight function, Hampel weight function and Tukey function. According to the experimental analysis, we choose the IGG (Institute of Geodesy and Geophysics) weight function [28]:

$$\bar{P} = \begin{cases} P_i & |V_i| < k_0 \\ P_i \cdot \frac{k_0}{|V_i|} \frac{(k_1 - |V_i|)^2}{(k_1 - k_0)^2} & k_0 \leq |V_i| < k_1 \\ 0 & k_1 \leq |V_i| \end{cases} \quad (32)$$

In this stage, two key issues need to be solved [31]. The first is the definition of k_0 and k_1 ; the second is the choice of weight. Generally, k_0 and k_1 are set as constant, e.g., $k_0 \in [1.0 \sim 1.5]$, $k_1 \in [3.0 \sim 8.0]$. If we consider the robust equation of both the parameter matrix and the observation space, the mean value of the number of redundant observations is $\sqrt{(n-m)/n}$; n and m are the numbers of observations and parameters, respectively. As a result, the value of k_0 and k_1 should be $k_0 = k_0' \cdot k$ and $k_1 = k_1' \cdot k$, where $k_0' \in [1.0 \sim 1.5]$, $k_1' \in [3.0 \sim 8.0]$, and $k = \sqrt{n/(n-m)}$. These initiatives make the selection of k_0 and k_1 vary with different n and m , increasing the flexibility of the robust estimation. Generally, the estimation of Equation (32) usually involves the iterative method; the iterative solution of step $t + 1$ should be

$$\widehat{X}_{kM}^{t+1} = (A_k^T \bar{P}^t A_k)^{-1} A_k^T \bar{P}^t L_k \quad (33)$$

4. Experiments and Discussion

To test the performance of the new GNSS single-epoch AR method, GPS/GLONASS/BDS real data of two stations (Sta1 and Sta2) for 24 hours on 3 March 2014, were collected. The length of the baseline between the stations was 9.5 m. The observation interval was 30 seconds. Moreover, the position of the two stations is exactly known. In this section, we first fix the ambiguity of the BDS triple-frequency signals and then realize the AR of GPS/GLONASS signals using the method proposed in this paper. Figure 2 shows the number of visible satellites of BDS and GPS/GLONASS. From Figure 2, we can see that there are 8–14 BDS visible satellites in the experimental period. For the GPS and GLONASS combined system, over 14 satellites can be used in the data processing.

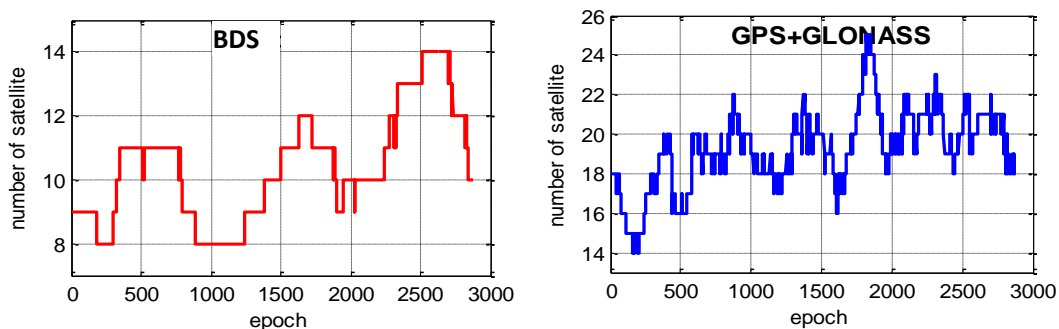


Figure 2. Number of visible satellites of BDS/GPS/GLONASS.

4.1. Ambiguity Resolution of BDS Triple-Frequency Signals

Due to the large wavelength, we can fix the ambiguity of the extra-wide-lane combination easily. In this study, the ambiguity of the BDS DD carrier phase observation is fixed based on Equation (25). Generally, the estimated ambiguity is more reliable when the difference between the float ambiguity and the integer is smaller. Figure 3 shows the distribution of the difference (DF) between float ambiguity and the integer of Geostationary Earth Orbit (GEO), Inclined Geosynchronous Satellite Orbit (IGSO) and Medium Earth Orbit (MEO) satellite observation. From this figure, we can see that more than 98% of the DF of the GEO satellites floats in the range of -0.2 to -0.1 cycles. Consequently,

using the rounding method to fix the ambiguity of GEO observation is reliable enough. For IGSO and MEO satellites, the DF mainly varies around ± 0.3 . However, some DF reach approximately 0.5 cycles. On this occasion, using the rounding method will result in mis-fixing. The reliability of the ambiguity resolution will be relatively low.

Generally, the difference between the float ambiguity and the integer is decided by the ionospheric delay and the noise of the DD carrier phase observation. This difference of GEOs is smaller than that of IGSOs, and MEOs mean that the noise of the GEO carrier phase observation is smaller than that of the other kinds of satellites. Similar results are also shown in the paper [32], revealing that the amplitudes of the ionosphere-free and geometry-free time series of GEOs is smaller than that of IGSOs' and MEOs' carrier phase measurement.

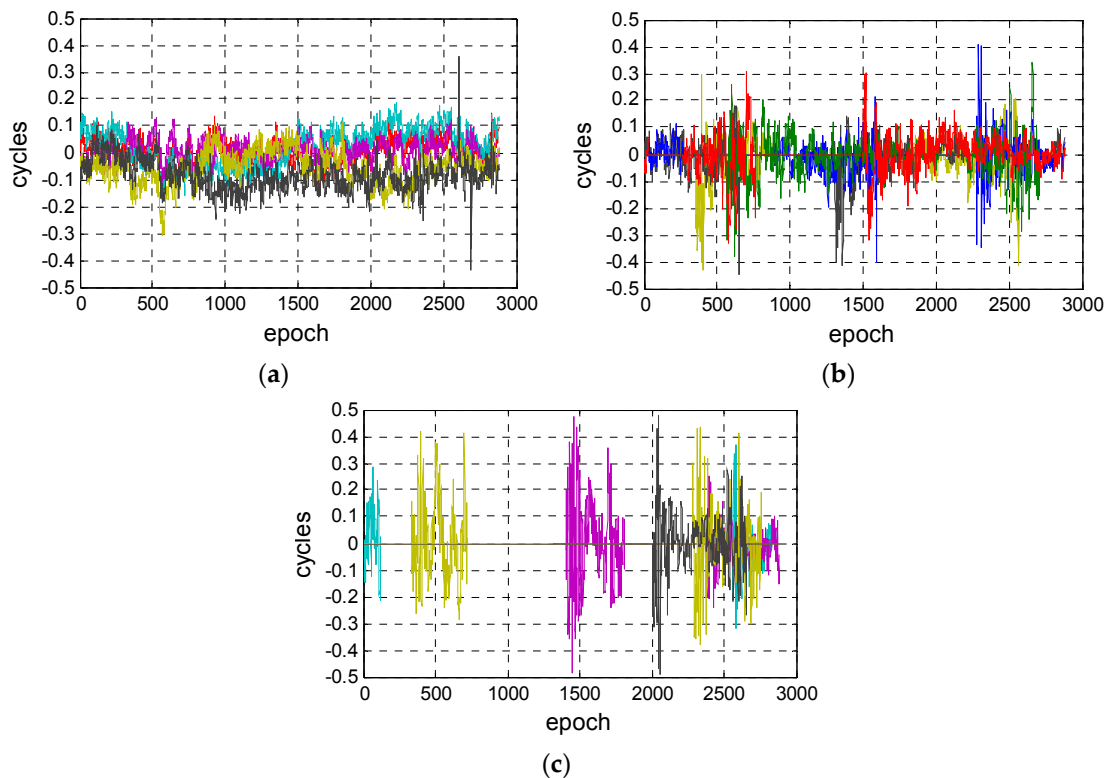


Figure 3. Variation of distribution of the difference (DF) of three kinds of BDS satellites. GEO = Geostationary Earth Orbit; IGSO = Inclined Geosynchronous Satellite Orbit; MEO = Medium Earth Orbit. (a) GEO; (b) IGSO; (c) MEO.

To verify the ambiguity at each epoch, we put the ambiguity into the DD ionosphere-free combination and simplify it as

$$V = A\hat{X} - L \quad (34)$$

The unknown parameter \hat{X} here includes the correction of the unknown coordinates δx , δy , δz , the zenith tropospheric delay, and the ambiguity. Based on the least-square estimation, we can measure the accuracy of the unknown parameter with the mean square error σ (Equation (34)).

$$\sigma = \pm \sqrt{\frac{[vv]}{n - t}} \quad (35)$$

In this equation, n represents the number of observations at each epoch, and t is the necessary number of observations. Figure 4 shows the variation of the absolute value of the mean square error at each epoch. The measurement noise of the ionosphere-free combination contributes most of the error

in Equation (34). In general, the carrier-phase measurement noise is ± 2 mm. According to the law of error propagation, the measurement noise of the ionosphere-free combination should be ± 1.2 mm, and the limit error should be 3.8 mm (3 times sigma). From Figure 4, we can see that the mean square error of some epochs is beyond 10 mm and the maximum reaches 53 mm. It is obvious that the integer AR at these epochs is wrong. The main reasons are that (1) the mis-fixing in the AR of the extra-wide lane and (2) the measurement noise and the ionospheric delay residual affect the AR of the BDS carrier phase observation.

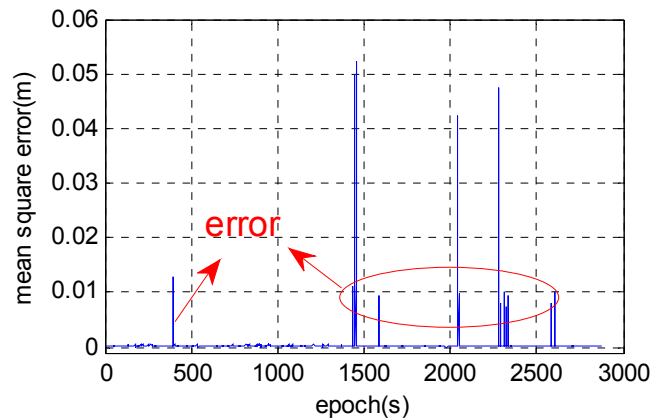


Figure 4. Variation of the absolute value of mean square error.

4.2. Ambiguity Resolution of GPS/GLONASS Signals

In this section, we fix the ambiguity of the GPS/GLONASS signals based on the BDS triple-frequency carrier phase observation with known ambiguity. To test the performance of the new method proposed in this study, we process the data using three schemes. The first one (S1) is using the new method to obtain the position of the rover; the second (S2) involves the robust estimation; and the third (S3) is the combined utilization of all instrument systems (GPS/GLONASS/BDS) with the three steps mentioned in Section 2. Before the data processing, the cycle slips were detected and repaired. In this section, we verify the ambiguity by comparing the estimated coordinate with the accurate coordinate. The ambiguity-fix rate (AFR) [33] was applied to quantify the efficiency performance of AR with the following definition:

$$\text{AFR} = \frac{\text{Number of epochs with ambiguity fixed to integer}}{\text{Total number of epochs observed in the data sets}} \quad (36)$$

Figures 5–7 display the deviation of the coordinate in the N, E, and U directions of the first two schemes. Figure a (Figures 5a, 6a and 7a) represents the result of least-squares estimation, and Figure b (Figures 5b, 6b and 7b) indicates the result of the robust estimation. From these figures, we can see that some epochs produce a big offset in three directions if we use the least-squares estimation directly. Some of the deviations even reach 1 m. Referring to Figure 3, which shows the resolution of BDS carrier-phase ambiguity, we find that the epochs with large coordinate deviation also have a large BDS mean square error. Thus, the wrong BDS ambiguity will result in an offset of the GPS/GLONASS AR model. Therefore, we can choose the BDS satellites with the correct ambiguity to restrict the calculation of the GPS/GLONASS ambiguity. However, it is difficult to obtain 100% correct BDS triple-frequency ambiguity due to measurement noise and other uncertain factors. To overcome these issues, we use robust estimation in the second scheme. Figure b (Figures 5b, 6b and 7b) show that the coordinate deviations in the N, E, and U directions are obviously smaller than those of Figure a (Figures 5a, 6a and 7a). Based on the robust estimation, the weight of the observation with outliers or mis-fixing ambiguities is reduced significantly and relatively high precise coordinates are obtained. Table 1 describes the distribution of coordinate deviation; 100% coordinate deviations of the second

scheme float in the range of ± 5 cm. It can be considered that all of the GPS/GLONASS ambiguity is resolved correctly.

Table 2 shows the AFR of S1 and S3. As shown in this table, we can fix the ambiguity in one epoch by using the new method proposed in this paper. However, five epochs are needed to accomplish the AR with S3.

There is one limitation of the method proposed in this paper. This method ignores the effect of the ionospheric and tropospheric delay and is limited to the short-range baseline. In another paper, we developed a new method to fix the ambiguity of GPS/BDS for a long-range baseline [26].

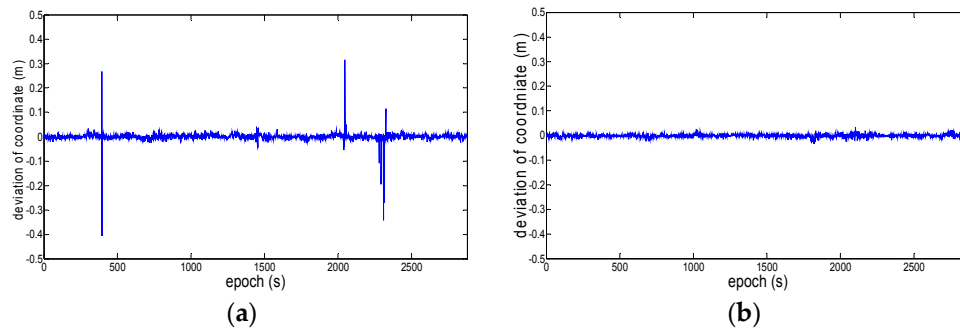


Figure 5. Deviation of coordinate (North). (a) without robust estimation; (b) with robust estimation.

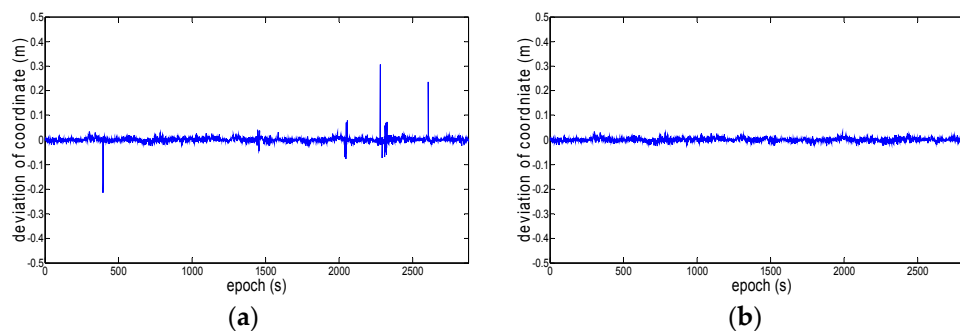


Figure 6. Deviation of coordinate (East). (a) without robust estimation; (b) with robust estimation.

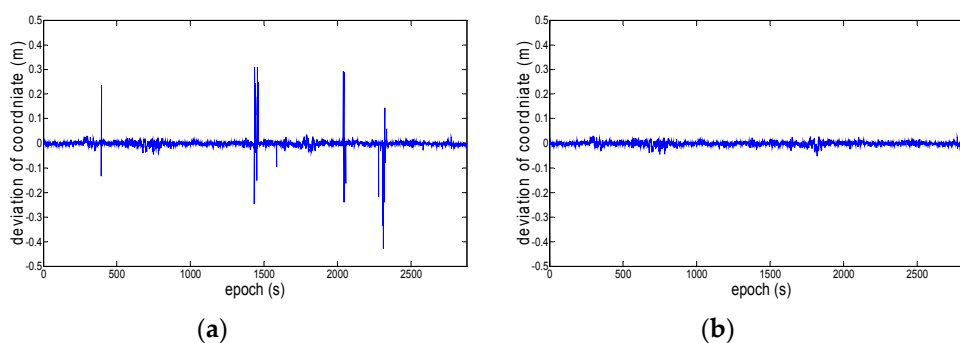


Figure 7. Deviation of coordinate (Up). (a) without robust estimation; (b) with robust estimation.

Table 1. The distribution of coordinate deviation (%).

	Without Robust Estimation			With Robust Estimation		
	0–0.03 cm	0.03–0.05 cm	>0.05 cm	0–0.03 cm	0.03–0.05 cm	>0.05 cm
North	99.0	0.2	0.8	99.9	0.1	0
East	99.0	0.5	0.5	99.9	0.1	0
Up	98.2	0.6	1.2	99.4	0.6	0

Table 2. Ambiguity-Fix Rate (AFR) of S1 and S3.

Time to Fix (epoch)	S1	S3
1	100.00%	97.53%
2		99.41%
3		99.65%
4		99.69%
5		100.00%

5. Conclusions

The development of GPS, BDS, GLONASS and Galileo marks a new era for our GNSS community. How to take advantage of multiple-frequency and multiple-constellation signals to improve the availability, reliability and accuracy of GNSS navigation and positioning service has become a research focus. This study focuses on the research of taking full advantage of every system and improving the efficiency of ambiguity resolution. A new single-epoch GNSS AR method for a short-range baseline based on triple-frequency signals is developed in this study. To test the performance of the new technique, real GPS/GLONASS/BDS data are processed. From the discussions above, we can obtain the conclusions below:

(1) Triple- or multiple-frequency signals can form an EWL and WL(Wide Lane) linear combination; their ambiguities can be fixed much more easily. The test results show that the AR of the GEOs' observation is more reliable than that of the MEO and IGSOs' observation by rounding the float ambiguities to integers.

(2) Using BDS carrier phase observation with known ambiguity to compute the prior information will not only enhance the dependability of the GNSS observation equation but also significantly increase the efficiency of the AR of GNSS double-frequency signals.

(3) Least squares with robust estimation can effectively resist the effect of the residual from the mis-fixing BDS ambiguity.

In conclusion, the new method can realize single-epoch GNSS AR for a short-range baseline based on triple-frequency signals.

This method is based on triple-frequency signals. Note that 20 BDS satellites are currently in operation: 6 GEOs, 8 IGSOs and 6 MEOs. The full constellation is scheduled to comprise 35 satellites. According to its overall planning schedule, a BDS Navigation Satellite System with global coverage will be in place by 2020. Consequently, customers in the Asia-Pacific region can use this method right now, and it will be available for global users by 2020.

Acknowledgments: This research was supported by the Scientific Research Foundation of Shandong University of Science and Technology for Recruited Talents (No. 22016RCJJ014) and Public Science and Technology Research Funds Projects of Surveying and Mapping (grant No. 201512034) and Natural Science Foundation of Fujian Province (project No.2015J01176).

Author Contributions: For this study, Shengli Wang, Xiushan Lu and Ying Xu conceived and designed the experiments; Shengli Wang and Jian Deng performed the experiments; Shengli Wang, Ying Xu and Ziyuan Song analysed the data; Shengli Wang and Ying Xu contributed analysis tools; Ying Xu and Ziyuan Song wrote the paper.

Conflicts of Interest: The authors declare no conflict of interest.

References

- Li, J.; Zhang, Y.; Wang, X.; Qin, Q.; Wei, Z.; Li, J. Application of GPS trajectory data for investigating the interaction between human activity and landscape pattern: A case study of the Lijiang River Basin, China. *ISPRS Int. J. Geo-Inf.* **2016**, *5*, 104. [[CrossRef](#)]
- Estima, J.; Painho, M. User Generated spatial content-integrator: Conceptual model to integrate data from diverse sources of user generated spatial content. *ISPRS Int. J. Geo-Inf.* **2016**, *5*, 183. [[CrossRef](#)]
- Leick, A. *GPS Satellite Surveying*; John Wiley & Sons: New York, NY, USA, 2004.

4. Parkinson, B.W. *Progress in Astronautics and Aeronautics: Global Positioning System: Theory and Applications*; AIAA: San Francisco, CA, USA, 1996.
5. Hatch, R. Ambiguity resolution while moving—experimental results. In Proceedings of the ION GPS, Albuquerque, NM, USA, 11 September 1991; Volume 91, pp. 10–13.
6. Hatch, R. Instantaneous ambiguity resolution. In *Kinematic Systems in Geodesy, Surveying, and Remote Sensing*; Springer: Berlin, Germany, 1991; pp. 299–308.
7. Chen, D. *Development of a Fast Ambiguity Search Filtering (FASF) Method for GPS Carrier Phase Ambiguity Resolution*; University of Calgary: Calgary, AB, Canada, 1997.
8. Teunissen, P.J.G. Least-squares estimation of the integer GPS ambiguities. In Proceedings of the Invited Lecture, Section IV Theory and Methodology, IAG General Meeting, Beijing, China, 6 August 1993.
9. Teunissen, P.J.G. A new method for fast carrier phase ambiguity estimation. In Proceedings of the IEEE Position Location and Navigation Symposium, Las Vegas, NV, USA, 11 April 1994; pp. 562–573.
10. Zumberge, J.F.; Heflin, M.B.; Jefferson, D.C.; Watkins, M.M.; Webb, F.H. Precise positioning for the efficient and robust analysis of GPS data from large networks. *J. Geophys. Res.: Solid Earth* **1997**, *102*, 5005–5017. [[CrossRef](#)]
11. Zou, X.; Ge, M.; Tang, W.; Shi, C.; Liu, J. URTK: Undifferenced network RTK positioning. *GPS Solut.* **2013**, *17*, 283–293. [[CrossRef](#)]
12. Li, W.; Teunissen, P.; Zhang, B.; Verhagen, S. Precise point positioning using GPS and Compass observations. In Proceedings of the China Satellite Navigation Conference (CSNC), Wuhan, China, 15 May 2013; pp. 367–378.
13. Ge, M.; Gendt, G.; Rothacher, M.; Shi, C.; Liu, J. Resolution of GPS carrier-phase ambiguities in precise point positioning (PPP) with daily observations. *J. Geod.* **2008**, *82*, 389–399. [[CrossRef](#)]
14. Li, X.; Zhang, X.; Ge, M. Regional reference network augmented precise point positioning for instantaneous ambiguity resolution. *J. Geod.* **2011**, *85*, 151–158. [[CrossRef](#)]
15. Feng, Y.M.; Rizos, C.; Higgins, M. Multiple carrier ambiguity resolution and performance benefits for RTK and PPP positioning services in regional areas. In Proceedings of the ION GNSS 20th International Technical Meeting of the Satellite Division, Fort Worth, TX, USA, 25 September 2007; pp. 25–28.
16. Vollath, U.; Birnbach, S.; Landau, H.; Fraile-Ordóñez, J.M.; Martin-Neira, M. Analysis of three-carrier ambiguity resolution (TCAR) technique for precise relative positioning in GNSS-2. In Proceedings of the Global Navigation Satellite Systems, European Symposium, Nashville, TN, USA, 15 September 1998.
17. Li, X.; Ge, M.; Dai, X.; Ren, X.; Fritsche, M.; Wickert, J.; Schuh, H. Accuracy and reliability of multi-GNSS real-time precise positioning: GPS, GLONASS, BeiDou, and Galileo. *J. Geod.* **2015**, *89*, 607–635. [[CrossRef](#)]
18. Li, X.; Zus, F.; Lu, C.; Dick, G.; Ning, T.; Ge, M.; Wickert, J.; Schuh, H. Retrieving of atmospheric parameters from multi-GNSS in real time: Validation with water vapor radiometer and numerical weather model. *J. Geophys. Res.: Atmos.* **2015**, *120*, 7189–7204. [[CrossRef](#)]
19. Hatch, R.; Jung, J.; Enge, P.; Pervan, B. Civilian GPS: The benefits of three frequencies. *GPS Solut.* **2000**, *3*, 1–9. [[CrossRef](#)]
20. Feng, Y.; Li, B. A benefit of multiple carrier GNSS signals: Regional scale network-based RTK with doubled inter-station distances. *J. Spat. Sci.* **2008**, *53*, 135–147. [[CrossRef](#)]
21. Li, B.; Feng, Y.; Shen, Y. Three carrier ambiguity resolution: Distance-independent performance demonstrated using semi-generated triple frequency GPS signals. *GPS Solut.* **2010**, *14*, 177–184. [[CrossRef](#)]
22. Ji, S.; Chen, W.; Ding, X.; Chen, Y.; Zhao, C.; Hu, C. Potential benefits of GPS/GLONASS/GALILEO integration in an urban canyon—Hong Kong. *J. Navig.* **2010**, *63*, 681–693. [[CrossRef](#)]
23. Geng, J.; Bock, Y. Triple-frequency GPS precise point positioning with rapid ambiguity resolution. *J. Geod.* **2013**, *87*, 449–460. [[CrossRef](#)]
24. Tang, W.; Deng, C.; Shi, C.; Liu, J. Triple-frequency carrier ambiguity resolution for Beidou navigation satellite system. *GPS Solut.* **2014**, *18*, 335–344. [[CrossRef](#)]
25. Julien, O.; Alves, P.; Cannon, M.E.; Zhang, W. A tightly coupled GPS/GALILEO combination for improved ambiguity resolution. In Proceedings of the European Navigation Conference (ENC-GNSS'03), Calgary, AB, Canada, 9 September 2003; pp. 1–14.
26. Xu, Y.; Ji, S.; Chen, W.; Weng, D. A new ionosphere-free ambiguity resolution method for long-range baseline with GNSS triple-frequency signals. *Adv. Space Res.* **2015**, *56*, 1600–1612. [[CrossRef](#)]
27. Xu, G. *GPS Theory, Algorithms and Applications*; Springer: Heidelberg, Germany, 2003; pp. 119–123.

28. Wanninger, L.; Wallstab-Freitag, S. Combined processing of GPS, GLONASS, and SBAS code phase and carrier phase measurements. In Proceedings of the ION GNSS, Fort Worth, TX, USA, 25 September 2007; pp. 866–875.
29. Zinoviev, A.E. Using GLONASS in combined GNSS receivers: Current status. In Proceedings of the ION GNSS, Long Beach, CA, USA, 13 September 2005; pp. 1046–1057.
30. Yang, Y.; Gao, W. Integrated navigation based on robust estimation outputs of multi-sensor measurements and adaptive weights of dynamic model information. *Geo-Spat. Inf. Sci.* **2005**, *8*, 201–204.
31. Yang, Y.; He, H.; Xu, G. Adaptively robust filtering for kinematic geodetic positioning. *J. Geod.* **2001**, *75*, 109–116. [[CrossRef](#)]
32. Xu, Y.; Ji, S. Data quality assessment and the positioning performance analysis of BeiDou in Hong Kong. *Surv. Rev.* **2015**, *47*, 446–457. [[CrossRef](#)]
33. Ji, S.; Wang, X.; Xu, Y.; Wang, Z.; Chen, W.; Liu, H. First preliminary fast static ambiguity resolution results of medium-baseline with triple-frequency beidou wavebands. *J. Navig.* **2014**, *67*, 1109–1119. [[CrossRef](#)]



© 2017 by the authors; licensee MDPI, Basel, Switzerland. This article is an open access article distributed under the terms and conditions of the Creative Commons Attribution (CC BY) license (<http://creativecommons.org/licenses/by/4.0/>).